ELSEVIER

www.elsevier.nl/locate/jorganchem

Journal of Organometallic Chemistry 595 (2000) 178–185

Journal of Organometallic Chemistry

Synthesis and structure of Rh(I) tris(pyrazolyl)borate complexes of the type $Tp^{Ph,Me}RhL_1L_2$

Monika Moszner [a,*] Stanisław Wołowiec [a,1], Alexander Trösch [b], Heinrich Vahrenkamp [b]

[a] *Faculty of Chemistry, University of Wrocław, F. Joliot-Curie Strasse 14, PL-50-383 Wrocław, Poland*
[b] *Institut für Anorganische und Analytische Chemie, Alberts-Ludwig Universität Freiburg, Albertstrasse 21, D-79104 Freiburg, Germany*

Received 17 August 1999; accepted 27 September 1999

Abstract

The complex $Tp^{Ph,Me}Rh(CO)_2$ (**1**) was prepared from the reaction of the appropriate potassium pyrazolyl borate, $Tp^{Ph,Me}K$, with $Rh(acac)(CO)_2$ in warm benzene. Reaction of $Rh(acac)(CO)_2$ with $Tp^{Ph,Me}K$ and PPh_3 gave the compound $Tp^{Ph,Me}Rh(CO)(PPh_3)$ (**2**). The complexes **1** and **2** were characterized by elemental analysis and IR, ^{1}H-, ^{13}C-, and ^{31}P-NMR spectroscopies. The structures of both compounds were determined by X-ray crystallography. The complex **1** crystallizes in the triclinic space group $P\bar{1}$ with $a = 11.227(2)$, $b = 12.219(2)$, $c = 12.262(2)$ Å, $\alpha = 63.61(3)$, $\beta = 87.67(3)$, $\gamma = 88.17(3)°$, $V = 1505.4(4)$ Å^3, and $Z = 2$. Crystals of **2** are triclinic, space group $P\bar{1}$, with $a = 11.114(2)$, $b = 11.913(2)$, $c = 18.071(4)$ Å, $\alpha = 82.69(3)$, $\beta = 82.02(3)$, $\gamma = 64.01°$, $V = 2123.9(7)$ Å^3, $Z = 2$. The fluxional behavior of **1** and **2** was studied by variable-temperature ^{1}H-NMR spectroscopy. In the case of **1** the $\kappa^2 \leftrightarrow \kappa^3$ conversion is fast on the NMR time-scale even at -90°C, whereas complex **2** is a unique example of two well-separated $\kappa^2 \leftrightarrow \kappa^3$ equilibria (by 21 kJ mol^{-1} $\Delta G^{\neq}$ gap).

Keywords: Rhodium; Pyrazolylborate complexes; NMR spectroscopy; Crystal structures

1. Introduction

The hydridotris(pyrazolyl)borate anion (Tp) has been demonstrated to be advantageous as a chelate ligand in organometallic and bioinorganic studies since Trofimenko's first report [1]. Studies on coordination chemistry of the first row of transition-metal complexes (Mn, Fe, Co, Ni, Cu and Zn) have led to the successful analysis of many aspects of biological systems like oxygen metabolism [2] and zinc-dependent bioinorganic reactions [3]. Throughout the last decade, synthetic studies have been extended to complexes of the second- and third-row transition metals. They contribute to a better understanding of the role of the central atoms in various catalytic and biological functions.

The Tp′ ligands, having various substituents at the pyrazolyl ring, are able to tune the electronic and steric environment of the central metal atoms. The tris(pyrazolyl)borates (Tp′) are normally tridentate ligands and usually coordinate in a tripodal fashion. However, the hapticity of Tp′ ligands in their complexes with transition-metal ions depends on both the steric requirements of Tp′ and of auxiliary ligands in $Tp'M(L)_n$, as well as on the metal ion (Scheme 1).

The phenyl substituent of the tris[3-phenyl,5-methylpyrazol-1-yl)borate ligand $Tp^{Ph,Me}$ possesses intermediate steric requirements in comparison with the small (3-H or 3-CH_3) or extremely high (3-^{t}Bu) steric hindrance of other 3-substituents [4], being comparable with 3-^{i}Pr or 3-*neo*-pent substituted Tp′ ligands [5].

The steric hindrance of the latter substituents led to borotropic rearrangement of one of the pyrazolyl rings in homoleptic $(Tp')_2Co$ complexes, and eventually the [HB(3-Rpz)$_2$(5-Rpz)]Co complexes were isolated and characterized both in solid state by X-ray diffraction and in solution by ^{1}H-NMR methods [5a,b]. In the case

* Corresponding author. Tel.: +48-71-3204228; fax: +48-71-3282348.
E-mail address: mm@wchuwr.chem.uni.wroc.pl (M. Moszner)
[1] Present address: Department of Chemistry, Polytechnical University of Rzeszów, 6, Powstańców Warszawy Ave., PL-35-959 Rzeszów, Poland.

0022-328X/00/$ - see front matter
PII: S0022-328X(99)00589-6

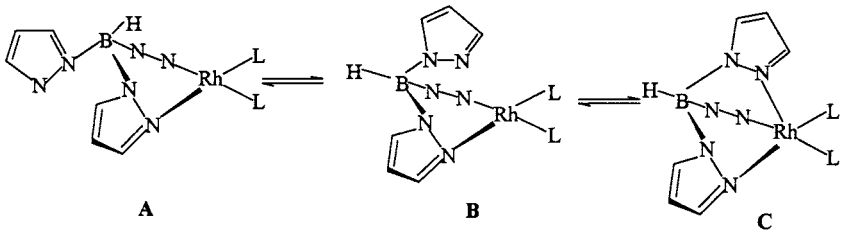

Scheme 1.

of Tp^{Ph} the pyrazole did not undergo a borotropic shift; instead the two Tp′ ligands were coordinated in a κ^3 and κ^2 fashion in the bis-ligand Co(II) complex [6]. Borotropic shift was also observed for $Tp^{iPr,4Br}$Rh-(COD) complex [7]. For comparison the Tp′ ligands with 3-R=H, CH_3, or thienyl substituents preferentially form bis-ligand Co(II) complexes, whereas mono-Tp′Co(II)X complexes are formed exclusively when R is the *t*-butyl group [4,8].

The denticity of poly(pyrazolyl)$_n$borate ligands can often differ from *n*, being e.g. $n-1$ for κ^2-bonded tris(pyrazolyl)borates, or $n+1$ for some types of bis-pyrazolylborates through participation of, e.g. agostic interaction [6,8c,9,10]. Very recently a new κ^2N,H bonding mode has been reported, where only one pyrazolyl ring is N-bound to rhodium, and the B-bound hydrogen interacts agostically with rhodium [10].

In the case of Tp′Rh(LL), the Tp′ ligands are mostly coordinated in κ^2 fashion to form 16-electron complexes although there are evidenced cases of 18-electron complexes with κ^3 bound Tp′ or related ligands in the solid state [11]. All Tp′Rh(LL) complexes show a fluxional behavior in solution due to the $\kappa^2 \leftrightarrow \kappa^3$ interconversion which has been extensively studied by NMR and IR spectral methods [11d,12,13]. Generally, the smaller the steric hindrance of Tp′ and auxiliary LL ligands is, the faster the interconversion takes place due to an easily available transition state with a κ^3 coordinated Tp′ ligand. In fact, in those cases, where the 3-substituent is H, CH_3, or CF_3, the complexes show fast exchange on the ^{1}H-NMR time-scale [11d,12]. On the other hand, in the case of larger 3-substituents and LL=COD, NBD fast exchange was also observed [11f]. Accordingly, it is difficult to predict the fluxional behavior of Tp′ ligands in κ^2-Tp′Rh(LL) complexes.

An upsurge of interest in the synthesis and characterization of rhodium complexes of hindered Tp′ ligands has stemmed from the discovery that hydridotris(pyrazolyl)borate rhodium complexes are able to activate the C–H and C–C bonds of hydrocarbons [14]. Ozawa and co-workers have found that Tp′Rh(COD) complexes exhibit high catalytic activity toward the polymerization of a variety of *para*-substituted phenylacetylenes [14h].

Here we report a new synthesis, structural and fluxional behavior studies of two Tp′Rh(LL) complexes containing a Tp′ ligand with intermediate steric hindrance imposed by 3-phenyl and 5-methyl substituents and two different sets of auxiliary LL ligands: LL = 2CO (**1**) and LL = CO, PPh_3 (**2**). The complex $Tp^{Ph,Me}Rh(CO)_2$ was obtained previously by bubbling CO through a solution of [RhCl(COD)], followed by the addition of $TlTp^{Ph,Me}$ [15], but it was not characterized in detail. The substitution of one carbonyl ligand in the former by triphenylphosphine was achieved by heating $[Tp^{Ph,Me}Rh(CO)_2]$ with PPh_3 to give $Tp^{Ph,Me}Rh(CO)(PPh_3)$ [12b]. None of these complexes has been investigated structurally so far.

We have prepared the complexes $Tp^{Ph,Me}Rh(CO)_2$ (**1**) and $Tp^{Ph,Me}(CO)(PPh_3)$ (**2**), using $Rh(acac)(CO)_2$ as the rhodium source. Both complexes contain the Tp′ ligand κ^2 coordinated in the solid state. The $\kappa^2 \leftrightarrow \kappa^3$ interconversion dynamics was studied by variable-temperature ^{1}H-NMR spectroscopy in solution. In the case of **1**, the $\kappa^2 \leftrightarrow \kappa^3$ conversion is fast on the NMR time-scale even at the lowest temperature available, whereas the low-symmetry complex **2** is a unique example of two well-separated $\kappa^2 \leftrightarrow \kappa^3$ equilibria (by 21 kJ mol^{-1} $\Delta G^{\neq}$ gap).

2. Experimental

2.1. Materials and instrumentation

$RhCl_3 \cdot 3H_2O$ was purchased from Aldrich. All solvents were reagent grade and were used as commercially available. The $KTp^{Ph,Me}$ salt was obtained according to the literature method [15].

Infrared spectra were measured in the range 4000–400 cm^{-1} as KBr disks on Bruker Vector 22 FT-IR and on FT-IR Nicolet Impact 400 spectrometers. The NMR spectra were recorded on a Bruker AMX-300 spectrometer (^{1}H at 300.1 MHz, ^{13}C at 75.5 MHz, ^{31}P at 121.5 MHz, and on a Bruker 200 MHz (^{1}H at 200.1 MHz, ^{31}P at 81.01 MHz) with TMS as internal standard for ^{1}H and ^{13}C, and 85% H_3PO_4 as external standard for ^{31}P.

2.2. Synthesis of $Tp^{Ph,Me}Rh(CO)_2$ (1)

$KTp^{Ph,Me}$ (0.11 g, 0.22 mmol) dissolved in 5 ml of warm benzene was added slowly to a solution of $Rh(acac)(CO)_2$ (0.05 g, 0.2 mmol) in 5 ml of benzene. The resulting mixture was stirred for 20 h at room temperature. The precipitated K(acac) was filtered off. The volume of the filtrate was reduced to 2 ml and the yellow solid was filtered off, washed with small portions of ethanol, diethyl ether and vacuum dried. Yield 52% (0.064 g). Anal. Found: C: 59.66; H, 4.44; N, 13.17. Anal. Calc. for $C_{32}H_{28}BN_6O_2Rh$: C, 59.84; H, 4.49; N, 13.1%.

IR: ν_{BH} 2516, ν_{CO} 2074, 2003 cm^{-1}. ^{1}H-NMR ($CDCl_3$): δ 2.48 s (9H, 5-CH_3), 6.26 s (3H, 4-H), 7.26–7.44 m (9H, *m*-, *p*-H), 7.86 d (6H, *o*-H) ppm; ^{13}C-NMR ($CDCl_3$): δ 184.6 ppm (d, CO), $J_{Rh,C} = 468$ Hz.

2.3. Synthesis of $Tp^{Ph,Me}Rh(CO)(PPh_3)$ (2)

The reaction was carried out under N_2 atmosphere. $KTp^{Ph,Me}$ (0.11 g, 0.22 mmol) dissolved in 5 ml of warm benzene was combined with $Rh(acac)(CO)_2$ (0.05 g, 0.2 mmol) in 5 ml of benzene. The reaction mixture was refluxed for 0.5 h. PPh_3 (0.052 g, 0.2 mmol) dissolved in 5 ml of hot benzene was added to the reaction mixture and the solution was refluxed for another 2 h. After cooling, K(acac) was filtered off. The yellow filtrate was evaporated in vacuo to give a thick, syrupy liquid. Addition of petroleum ether (fraction 60–70°C) and stirring for 1 h resulted in precipitation of a pale-yellow solid, which after filtration and washing with pentane was vacuum dried. Yield 74% (0.140 g). A modified procedure was also applied, in which the K(acac) side-product was separated before addition of PPh_3. In that case the yield was lower (32%).

Anal. Found: C, 66.54; H, 4.91; N, 9.58. Anal. Calc. for $C_{49}H_{43}BN_6OPRh$: C, 67.14; H, 4.94; N, 9.59%.

IR: ν_{BH} 2488, ν_{CO} 1983 cm^{-1}. ^{1}H-NMR (CD_2Cl_2): δ 2.21 s (6H, 5-CH_3), 2,56 s (3H, 5-CH_3), 6.0 s (2H, 4-H), 6.45 s (1H, 4-H), 7.0–7.18 (15H, PPh_3), 7.44–7.58 m (9H, *m*-, *p*-H), 8.32 d (6H, *o*-H) ppm. ^{31}P-NMR ($CDCl_3$) δ: 42.39 ppm d ($J_{Rh-P} = 164$ Hz). ^{13}C-NMR (CD_2Cl_2): δ 184.6 ppm (d, CO), $J_{Rh,C} = 492$ Hz.

2.4. Structure determination

Orange single crystals of **1** were obtained by slow evaporation from tetrahydrofuran–ethanol solution whereas yellow crystals of **2** were obtained from a chloroform–ethanol mixture.

Diffraction data were recorded with $\omega/2\theta$ technique on a Nonius CAD4 diffractometer fitted with a molybdenum tube (K_α, $\lambda = 0.7107$ Å) and a graphite monochromator at 293 K. No absorption corrections were applied. The structures were solved via the Patterson function for **1** and with direct methods for **2** and refined anisotropically with the SHELX program suite [16]. Hydrogen atoms were included with fixed distances and isotropic temperature factors 1.2 times those of their attached atoms. Parameters were refined against F^2. The R values are defined as $R_1 = \Sigma F_o - F_c / \Sigma F_o$ and $wR_2 = \{\Sigma[w(F_o^2 - F_c^2)^2 / \Sigma[w(F_o^2)^2]\}^{1/2}$. Drawings were produced with SHAKAL [17]. Table 1 lists the crystallographic details.

3. Results and discussion

3.1. Synthesis of $Tp^{Ph,Me}Rh(CO)_2$ (1) and $Tp^{Ph,Me}Rh(CO)(PPh_3)$ (2)

The complexes were obtained by treatment of $Rh(acac)(CO)_2$ with $KTp^{Ph,Me}$ for **1** and $KTp^{Ph,Me}$ and PPh_3 for **2** in benzene, according to Eqs. (1) and (2)

$$Rh(acac)(CO)_2 + KTp^{Ph,Me} \xrightarrow{C_6H_6} Tp^{Ph,Me}Rh(CO)_2 + K(acac) \quad (1)$$

$$Rh(acac)(CO)_2 + KTp^{Ph,Me} + PPh_3 \xrightarrow[\Delta]{C_6H_6} Tp^{Ph,Me}Rh(CO)(PPh_3) + K(acac) \quad (2)$$

It has been found that the yield of **2** depends on the reaction procedure. One-step synthesis (Eq. (2)) results in the higher yield, vide supra.

3.2. X-ray crystal structures of 1 and 2

Figs. 1 and 2 show the structures of the complexes, $Tp^{Ph,Me}Rh(CO)_2$ (**1**) and $Tp^{Ph,Me}Rh(CO)(PPh_3)$ (**2**), respectively. Selected bond lengths and angles are listed in Tables 2 and 3. The geometry about the rhodium atoms is square planar, the donors being two nitrogen atoms of the tris(pyrazolyl)borate anion and the two carbonyl ligands coordinated to the Rh atom for **1** and two nitrogen atoms of the $Tp^{Ph,Me}$ anion, one carbonyl group and one triphenylphosphine ligand for **2**. Although the rhodium coordination environment of both complexes is quite similar, there are some differences in the overall structures of **1** and **2**. The Rh–C distances are identical at 1.851(3) Å in **1**, while the Rh–C distance is 1.831(3) Å in **2**. The Rh–N separations are 2.098(2), 2.102(2) and 2.099(2), 2.120(2) Å for **1** and **2**, respectively. The Rh–N bond length *trans* to CO is longer than that *trans* to phosphorus in **2**. The Rh–P distance of 2.2683(10) Å in **2** is similar to that reported for $Tp^{Me_2}Rh(CO)(PPh_3)$–2.272(2) Å [12b]. The Rh–N(3) separation of the uncoordinated pyrazole is 2.835 Å in **1** and 3.664 Å in **2**. The geometry and bond lengths for the presently reported $Tp^{Ph,Me}Rh(CO)_2$ complex are comparable to those found in the complex $Tp^aRh(CO)_2$ (Rh–N, 2.09; Rh···N, 2.78; Rh–C, 1.85 Å) (Tp^a =

Table 1
Crystal and data collection parameters for $Tp^{Ph,Me}Rh(CO)_2$ and $Tp^{Ph,Me}Rh(CO)(PPh_3)$

	1	**2**
Compound name	Dicarbonyl-rhodium(I)-(*N*,*N*)tris-(3-methyl-5-phenyl-pyrazolyl-1-yl)borate	Carbonyl(trisphenylphosphine)rhodium(I)tris-(3-methyl-5-phenylpyrazol-1-yl)borate
Empirical formula	$C_{32}H_{28}BN_6O_2Rh$	$C_{49}H_{43}BN_6OPRh$
Formula weight	642.3	876.6
Crystal system, space group	Triclinic; $P\bar{1}$	Triclinic; $P\bar{1}$
Unit cell dimensions		
a (Å)	11.227(2)	11.114(2)
b (Å)	12.219(2)	11.913(2)
c (Å)	12.262(2)	18.071(4)
α (°)	63.61(3)	82.69(3)
β (°)	87.67(3)	82.02(3)
γ (°)	88.17(3)	64.01(3)
V (Å^3)	1505.4(4)	2123.9(7)
Z	2	2
$D_{calc.}$ (g cm^{-3})	1.417	1.371
Absorption coefficient (mm^{-1})	0.606	0.485
$F(000)$	656	904
Crystal size (mm)	$0.6\times0.5\times0.5$	$0.8\times0.7\times0.7$
Index ranges	$-13\le h\le13,\ 0\le k\le15,\ -13\le l\le15$	$-13\le h\le13,\ -14\le k\le14,\ 0\le l\le22$
Reflections collected/unique	6172/5881 [$R_{int}=0.0186$]	8612/8336 [$R_{int}=0.0509$]
Reflections observed	5199 [$I>2\sigma(I)$]	7080 [$I>2\sigma(I)$]
Data/restraints/parameters	5881/0/379	8336/0/532
Goodness-of-fit on F^2	1.068	1.065
Final R indices [$I>2\sigma(I)$]	$R_1=0.0381,\ wR_2=0.1065$	$R_1=0.0412,\ wR_2=0.1088$
R indices (all data)	$R_1=0.0472,\ wR_2=0.1141$	$R_1=0.0557,\ wR_2=0.1185$

hydrotris(2H - benz[9] - 4,5 - dihydroindazol - 2 - yl)borate [15] and $Tp^{CF_3,Me}(CO)_2$ [12a] (2.11, 2.64 and 1.83 Å, respectively). The molecular structure and bonding parameters of $Tp^{Ph,Me}Rh(CO)(PPh_3)$ are in line with those found for $(Tp^{Me_2})Rh(CO)(PPh_3)$ (Rh–N, 2.11; Rh···N, 3.537; Rh–P., 2.272; Rh–C, 1.824 Å) [12b].

3.3. IR spectral characteristics

The ν(CO) and ν(BH) stretching vibrations of complexes **1** and **2** are given in Table 4. The IR spectrum of **1** in $CHCl_3$ exhibits four overlapping carbonyl bands of almost the same intensities at 2089, 2077, 2022 and 2008 cm^{-1}, whereas only two bands are observed in the solid state at 2074 and 2003 cm^{-1}. Similarly, two $\nu_{(B-H)}$

Table 2
Selected distances (Å) and angles (°) with estimated S.D. for $Tp^{Ph,Me}Rh(CO)_2$ (**1**)

Bond distances			
Rh(1)–C(31)	1.851(3)	C(31)–O(1)	1.124(4)
Rh(1)–C(32)	1.851(3)	C(32)–O(2)	1.134(4)
Rh(1)–N(1)	2.098(2)	N(4)–B(1)	1.557(4)
Rh(1)–N(2)	2.102(2)	N(5)–B(1)	1.537(4)
Rh(1)–N(3)	2.835(2)	N(6)–B(1)	1.536(4)
Bond angles			
C(31)–Rh(1)–C(32)	86.91(15)	C(1)–N(4)–B(1)	129.0(2)
C(31)–Rh(1)–(N(1)	94.08(13)	N(1)–N(4)–B(1)	121.1(2)
C(32)–Rh(1)–N(1)	172.26(11)	C(11)–N(5)–B(1)	127.8(3)
C(31)–Rh(1)–N(2)	178.95(12)	N(2)–N(5)–B(1)	122.2(2)
C(32)–Rh(1)–N(2)	92.16(12)	N(3)–N(6)–B(1)	120.7(2)
N(1)–Rh(1)–N(2)	86.79(10)	N(6)–B(1)–N(5)	111.1(2)
C(3)–Rh(1)–N(1)	132.4(2)	N(6)–B(1)–N(4)	111.3(2)
N(4)–N(1)–Rh(1)	119.51(18)	N(5)–B(1)–N(4)	108.0(2)

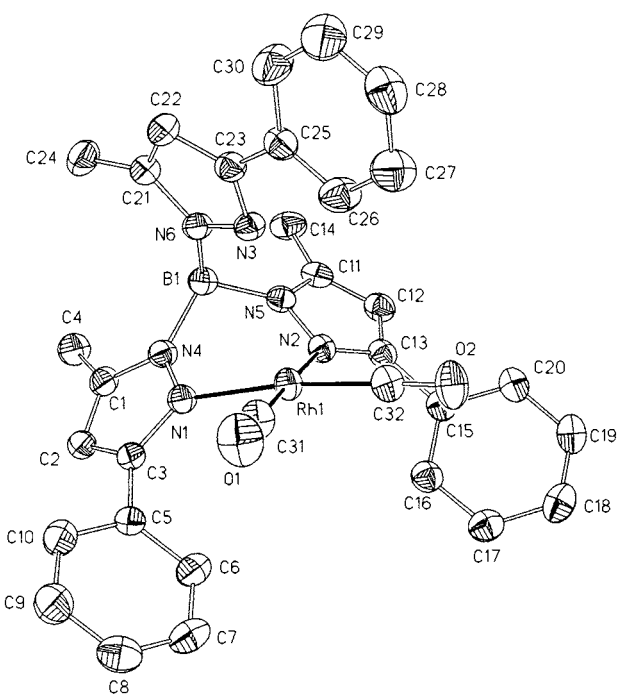

Fig. 1. Molecular structure of $Tp^{Ph,Me}Rh(CO)_2$

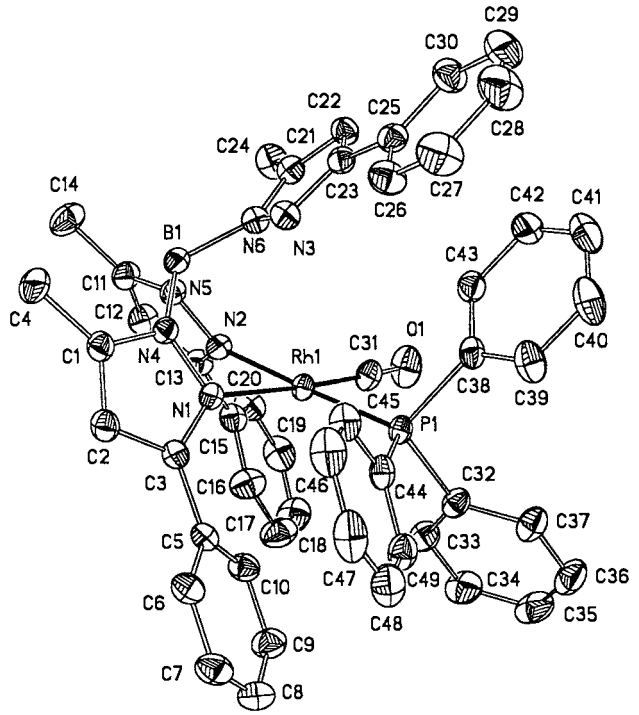

Fig. 2. Molecular structure of $Tp^{Ph,Me}Rh(CO)(PPh_3)$.

Table 3
Selected distances (Å) and angles (°) with estimated S.D. for $Tp^{Ph,Me}Rh(CO)(PPh_3)$ (**2**)

Bond distances			
Rh(1)–C(31)	1.813(3)	C(31)–O(1)	1.145(4)
Rh(1)–N(2)	2.099(2)	N(4)–B(1)	1.539(4)
Rh(1)–N(1)	2.120(2)	N(5)–B(1)	1.546(4)
Rh(1)–P(1)	2.2683(10)	N(6)–B(1)	1.551(4)
Rh(1)–N(3)	3.664		
Bond angles			
C(31)–Rh(1)–N(2)	91.16(12)	N(4)–N(1)–Rh(1)	116.45(17)
C(31)–Rh(1)–N(1)	174.25(11)	C(13)–N(2)–Rh(1)	134.4(2)
N(2)–Rh(1)–N(1)	83.14(9)	N(5)–N(2)–Rh(1)	118.22(18)
C(31)–Rh(1)–P(1)	87.49(10)	C(1)–N(4)–B(1)	126.9(3)
N(2)–Rh(1)–P(1)	177.98(7)	N(1)–N(4)–B(1)	121.8(2)
N(1)–Rh(1)–P(1)	98.19(7)	C(11)–N(5)–B(1)	129.9(3)
C(44)–P(1)–Rh(1)	118.99(10)	N(2)–N(5)–B(1)	120.5(2)
C(32)–P(1)–Rh(1)	113.03(11)	C(21)–N(6)–B(1)	128.4(2)
C(38)–P(1)–Rh(1)	113.75(11)	N(3)–N(6)–B(1)	118.5(2)
C(3)–N(1)–Rh(1)	136.23(19)		

bands are present in the IR spectrum of **1** in solution (2531 and 2489 cm^{-1}) and only one $\nu_{(B-H)}$ vibration at 2516 cm^{-1} is observed in solid state. It has been shown that both $\nu_{(B-H)}$ and $\nu_{(C-O)}$ stretching vibration frequencies can be used as a criterion of the coordination mode of Tp′ ligand [11a,12a,13a]. In particular, the presence of four $\nu_{(C-O)}$ bands in the IR spectra of $Tp'Rh(CO)_2$ complexes in solution has been demonstrated to indicate the contribution of two different isomers [12a,13a]. Unlike in the case of **1**, the IR spectrum of **2** consists of one $\nu_{(B-H)}$ and $\nu_{(C-O)}$ band both in solution and in solid state.

*3.4. Fluxional behavior of **1** and **2** as studied by ^{1}H-NMR spectroscopy*

Both complexes **1** and **2** contain the $Tp^{Ph,Me}$ ligand coordinated to Rh(I) in the κ^2 fashion in solid state. The ^{1}H-NMR examination of complex **1** in CD_2Cl_2 solution showed fast $\kappa^2 \leftrightarrow \kappa^3$ interconversion even at the lowest temperature available (Fig. 3). The spectrum consists of one set of 4-H and 5-CH_3 resonances over the whole temperature range studied (180–300 K).

The ^{1}H-NMR spectrum of **2**, containing the same Tp′ ligand and bulky PPh_3 in place of one CO, taken at room temperature, consists of two well-resolved sets of pyrazole ring resonances of 2:1 integral intensity ratio (Fig. 4). Lowering the temperature of CD_2Cl_2 (and toluene-d_9) solutions of **2** results in broadening and then splitting of the 5-CH_3 proton signal at 2.24 ppm as well as of the 4-H pyrazole resonance at 6.03 ppm into two pairs of separate signals, eventually leading to a spectrum in which three 4-H and three 5-CH_3 resonances are observed (bottom trace in Fig. 4). Simultaneously, the phenyl resonances of PPh_3 within the 6.4–7.4 ppm region lose their chemical equivalence.

The full assignment of the 4-H and 5-CH_3 resonances has been done based upon 2-D NOESY ^{1}H-NMR experiments performed for toluene-d_9 solutions of **2** at

Table 4
CO and B–H stretching vibrations (cm^{-1}) of **1** and **2**

Complex	CO		BH
	ν_{sym}	ν_{aym}	
$Tp^{Ph,Me}Rh(CO)_2$ (**1**)	2074 vs [a]	2003 vs	2516 m [a]
	2089 vs (sh) [b]	2022 vs (sh)	2531 m [b]
	2077 vs	2008 vs	2489 m
$Tp^{Me_2}Rh(CO)_2$ [c]	2055 vs [a]	1980 vs	
	2108 w [b]	2073 sh	
$Tp^{CF_3,Me}Rh(CO)_2$ [c]	2082 vs [a]	2016 vs	
	2100 s [b]	2037 s	
$Tp^{CF_3,CF_3}Rh(CO)_2$ [c]	2096 vs [a]	2038 vs	2083 w
	2110 m [b]	2051 m.	2051 vs
$Tp^{Me}Rh(CO)_2$ [d]	2061 [a]	1981	2012 s
	2085 s [b]	2019 s	1972 vs
$Tp^{iPr,4Br}Rh(CO)_2$ [d]	2074 [a]	2013	2001 br
	2089 vs [b]	2026 vs	
$Tp^{Ph,Me}Rh(CO)(PPh_3)$ (**2**)	1982 vs [a]		2488 m [a]
	1987 vs [b]		2482 m [b]

[a] KBr.
[b] $CHCl_3$.
[c] See Ref. [12a].
[d] See Ref. [11d].

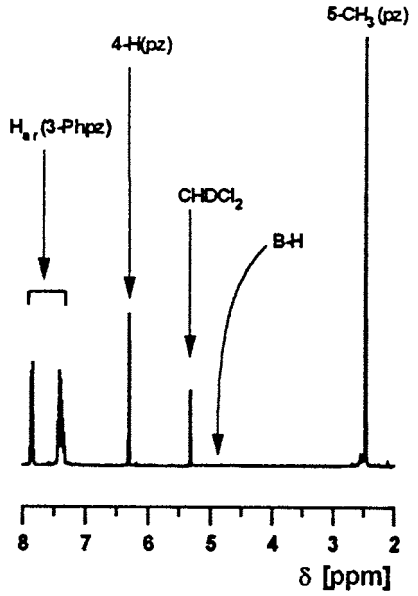

Fig. 3. ^{1}H-NMR spectrum of **1** in CD_2Cl_2 at 294 K.

234 and 217 K. The NOESY spectrum at 217 K shows NOE correlations between 4-H and 5-CH_3 of all three pyrazole rings. Additionally, NOE cross-peaks are observed between the 4-H and *o*-H (5-Ph(pz)) protons for coordinated pyrazoles and additionally between two 5-CH_3 of dangling and one of coordinated pyrazoles.

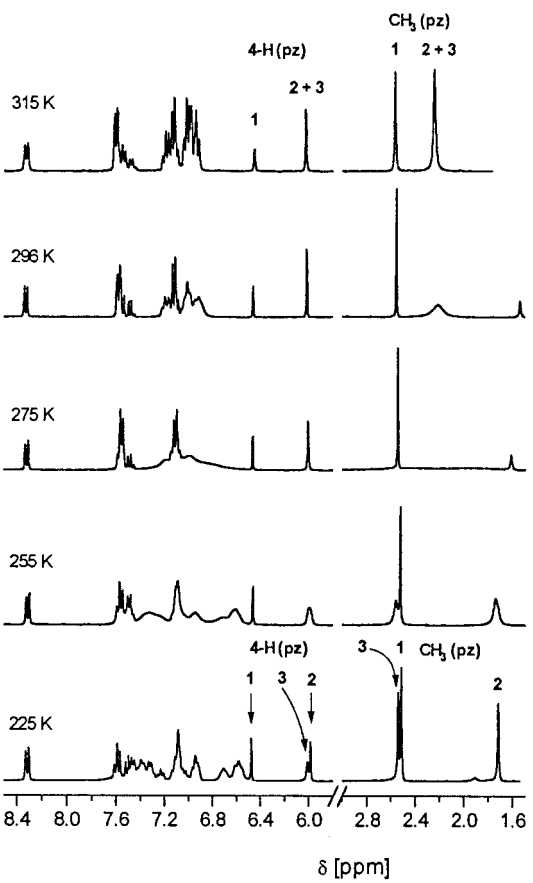

Fig. 4. Variable-temperature ^{1}H-NMR spectra of **2** in CD_2Cl_2. For labeling see Fig. 5.

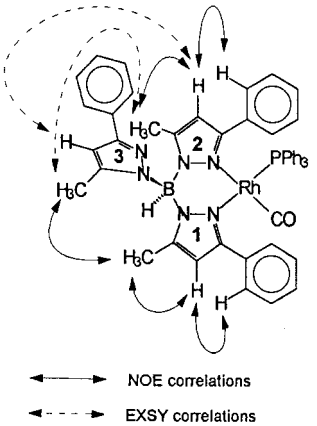

Fig. 5. Connectivity scheme within the molecule of **2** based on 2-D ^{1}H-NMR NOESY measurements in toluene-d_9 at 217 and 234 K.

Characteristically the 5-CH_3 resonance of uncoordinated pyrazole is shifted downfield the most, whereas the corresponding 4-H resonance is shifted upfield the most if compared with those of the coordinated pyrazole rings. The NOESY spectrum recorded at 234 K is dominated by strong EXSY peaks, two of which are of particular importance, i.e. those between the uncoordinated and one of the coordinated pyrazoles in the region of the 4-H and 5-CH_3 signals. The scheme of observed NOE and EXSY connectivities is presented in Fig. 5. The assignment of coordinated pyrazole resonances 1 and 2 deserves further comments, which will follow this section. Both the 4-H and 5-CH_3 signals labeled as 2 and 3 broaden upon increasing temperature and eventually the methyl resonances coalesce at 280 K, together with the averaging of phosphine phenyl resonances. The upper trace in Fig. 4 shows the spectrum of **2** taken at 315 K in CD_2Cl_2 solution, which reveals the sharp 2:1 pattern for all 4-H, 5-CH_3, *o*-H(3-Phpz), and phenyl(PPh_3) resonances.

The observed dynamic behavior is interpreted as an exchange between uncoordinated and CO-*trans* coordinated pyrazoles of the Tp′ ligand (Fig. 4). Selective exchange of coordinated pyrazole 2 was assumed because (i) fast exchange of all pyrazoles was observed previously for **1**, which bears two CO auxiliary ligands; (ii) the steric hindrance between the phenyl rings of PPh_3 and *cis*-coordinated $pz^{Ph,Me}$ destabilizes the Rh–N(pz) bond in *cis* position to Rh–P; (iii) the CO ligand possesses a stronger *trans* effect than PPh_3 [18]; and (iv) indeed, the Rh–N (pz) distance, *trans* to CO is distinctly larger than the one *trans* to P (phosphine) (see Table 3), analogous to the situation found for the complex $Tp^{Me_2}Rh(CO)(PPh_3)$ [12b]. However, when PPh_3 was replaced by PMe_3 in the latter complex, the

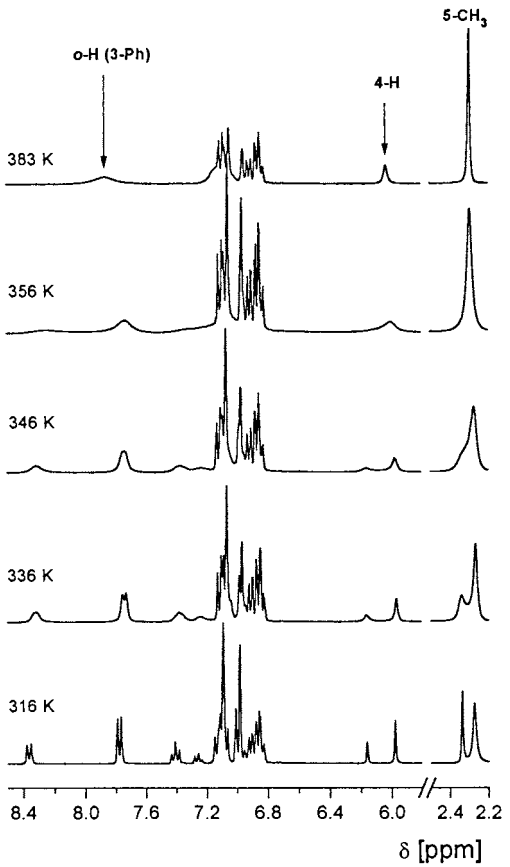

Fig. 6. Variable-temperature ^{1}H-NMR spectra of **2** in toluene-d_9.

2:1 pattern of the low-temperature ^{1}H-NMR spectrum was interpreted by an exchange between the pyrazole coordinated *trans* to PMe_3 and the dangling one, via a κ^3 five-coordinated intermediate, consistently with X-ray structural data [13c].

To further study the dynamics of the complex **2** we have performed high-temperature ^{1}H-NMR measurements in toluene-d_9 (Fig. 6). Upon increasing the temperature, the averaged spectrum of all pyrazoles was reached at 380 K (upper trace) with a coalescence temperature of 370 K. At this point the system remains in fast exchange on the ^{1}H-NMR time-scale, a situation which is achieved for **1** at a temperature more than 100° lower. Thus, we were able to observe the unique case of consecutive exchange between two coordinated and uncoordinated pyrazoles of the Tp′ ligand presumably mediated by a κ^3 five-coordinated intermediate as summarized in Scheme 1. The $\Delta G^{\neq}$ values, estimated from the coalescence temperatures for the $pz_2 \leftrightarrow pz_3$ and $pz_1 \leftrightarrow pz_3$ exchanges, are 55.0 and 76.5 kJ mol^{-1}, respectively. The latter value is higher than that found for $Tp^{Me_2}Rh(CO)(PMe_3)$ [13c] and $TpRh(C_2H_4)(PPh_3)$ [13b] (63 and 60 kJ mol^{-1}, respectively), with less-hindered Tp′ ligands.

It is noteworthy that in **2** as well as in both $Tp^{Me_2}Rh(CO)(PMe_3)$ and $TpRh(C_2H_4)(PPh_3)$ complexes containing κ^2-coordinated Tp′ ligands and their intermediates with the Tp′ coordinated in κ^3 fashion, the boron-centered chirality is generated due to the presence of two different ancillary ligands, one of which being phosphine in all cases. In the present case enantiomers of **2** are present in the solid state as a racemate within the unit cell. The $\kappa^2 \leftrightarrow \kappa^3$ interconversion in solution is accompanied by inversion of configuration at boron. Similar boron-centered chirality was achieved in the $Tp^{Mementh}Rh(CO)_2$ complex, ($Tp^{Mementh}$ = hydrotris(7(*S*)-*tert*-butyl-4(*R*)-methyl-4,5,6,7-tetrahydro-indazolyl) due to homochiral substituents on the pyrazole rings [13a]. In that case the dynamic features observed by means of ^{1}H-NMR spectroscopy were interpreted in terms of interconversion between form A, with axial B–H and equatorial uncoordinated pyrazole, revealing three chemically unequivalent pyrazole rings and two forms B and C (Scheme 1), namely κ^2-$Tp^{Mementh}Rh(CO)_2$ with axial uncoordinated pyrazole and κ^3-$Tp^{Mementh}Rh(CO)_2$, respectively, revealing fast B↔C exchange, with one averaged 5-H(pz) resonance. Forms A and B↔C were populated in a 80:20 ratio based on the IR spectrum. In that system the total averaging of all pyrazole resonances was achieved at 349 K, which gave a $\Delta G^{\neq}$ value of 66.4 kJ mol^{-1}. The A, B, and C forms (Scheme 1) were also postulated to explain the dynamic pattern of the complexes $Tp^{Me}Rh(COD)$ and $Tp^{iPr,4Br}Rh(COD)$ observed by ^{1}H-NMR measurements [7].

Actually, boron-centered chirality is present in all complexes of the Tp′RhL_1L_2 type (with $L_1 \neq L_2$), which has not been discussed, presumably due to the fact that the enantiomers could not be distinguished by spectral methods without converting them into diastereomers by complexation with other optically active reagents. Our attempts to form associates of **2** with brucine at low-temperatures, followed by ^{1}H-NMR spectroscopy did not show any spectral changes in the system in question. Thus, introducing a chiral substituent instead of hydrogen on boron seems to be necessary to achieve spectral distinction between the *R* and *S* configurations on boron in Tp′RhL_1L_2 complexes.

4. Concluding remarks

The $Tp^{Ph,Me}Rh(LL)$ complexes **1** and **2** were studied, with LL = 2CO and LL = CO, PPh_3, respectively. In the solid state both of them contain κ^2 coordinated Tp′ ligands. The replacement of one of the CO ligands by PPh_3 dramatically slows down the $\kappa^2 \leftrightarrow \kappa^3$ interconversion in **2** in comparison with that in **1**. The ^{1}H-NMR spectral studies showed that selective exchange between uncoordinated and *trans*-to-CO coordinated pyrazoles

occurs at temperatures above 280 K, whereas the second pyrazole, coordinated *trans*-to-PPh_3, exchanges with the uncoordinated one above 370 K. These two dynamic processes are discriminated by an energetic gap of 21.5 kJ mol^{-1} which results both from the difference in the *trans* effects of the two auxillary ligands (CO versus PPh_3) and from the steric hindrance between PPh_3 and the 3-phenyl substituent of the *cis*-coordinated pyrazole of Tp′.

5. Supplementary material

Tables of crystal of crystal data, structure refinement details, atomic coordinates, bond lengths and angles, anisotropic displacement parameters, and hydrogen coordinates are available from the Cambridge Crystallographic Data Centre with the following numbers: CCDC 133924 (**1**); CCDC 133925 (**2**).

Acknowledgements

This research has been supported in part by grants (M.M.) from the Deutscher Akademischer Austauschdienst (no. 6197-A9716962) and the Polish State Committee for Scientific Research (no. 3T09A 005 10).

References

[1] S. Trofimenko, J. Am. Chem. Soc. 88 (1966) 1842.
[2] (a) R. Czernuszewicz, J.E. Sheats, T.G. Spiro, Inorg. Chem. 26 (1987) 2063. (b) N. Kitajima, K. Fujisawa, Y. Moro-oka, J. Am. Chem. Soc. 111 (1989) 8975. (c) J. Egan, B.S. Haggerty, A.L. Rheingold, S.C. Sendlinger, K.H. Theopold, J. Am. Chem. Soc. 112 (1990) 2445, (d) N. Kitajima, H. Fukui, Y. Moro-oka, Y. Mizuyani, T. Kitagawa, J. Am. Chem. Soc. 112 (1990) 6402. (e) N. Kitajima, U.P. Singh, H. Amagai, M. Osawa, Y. Moro-oka, J. Am. Chem. Soc. 113 (1991) 7757. (f) N. Kitajima, M. Osawa, M. Tanaka, Y. Moro-oka, J. Am. Chem. Soc. 113 (1991) 8952. (g) N. Kitajima, K. Fujisawa, C.C. Fujimoto, Y. Moro-oka, S. Hashimoto, T. Kitagawa, K. Toriumi, K. Tatsumi, A. Nakamura, J. Am. Chem. Soc. 14 (1992) 1277. (h) S. Hikichi, H. Komatsuzaki, N. Kitajima, M. Akita, M. Mukai, T. Kitagawa, Y. Moro-oka, Inorg. Chem. 36 (1997) 266. (i) S. Hikichi, H. Komatsuzaki, M. Akita, Y. Moro-oka, J. Am. Chem. Soc. 120 (1998) 4699.
[3] (a) R. Alsfasser, S. Trofimenko, A. Looney, G. Parkin, H. Vahrenkamp, Inorg. Chem. 30 (1991) 4098. (b) K. Weis, M. Rombach, H. Vahrenkamp, Inorg. Chem. 37 (1998) 2470. (c) K. Weis, M. Rombach, M. Ruf, H. Vahrenkamp, Eur. J. Inorg. Chem. (1998) 263. (d) K. Weis, H. Vahrenkamp, Eur. J. Inorg. Chem. (1998) 271. (e) A. Trösch, H. Vahrenkamp, Eur. J. Inorg. Chem. (1998) 827. (f) P. Ghosh, T. Hascall, G. Parkin, Inorg. Chem. 36 (1997) 5680. (g) P. Ghosh, G. Parkin, J. Chem. Soc. Dalton Trans. (1998) 2281.
[4] S. Trofimenko, Chem. Rev. 93 (1993) 943.
[5] (a) S. Trofimenko, J.C. Calabrese, P.J. Domaille, G.S. Thompson, Inorg. Chem. 28 (1992) 1091. (b) J.C. Calabrese, S. Trofimenko, Inorg. Chem. 31 (1992) 4810.
[6] A. Kremer-Aach, W. Kläui, R. Bell, A. Sterath, H. Wunderlich, D. Mootz, Inorg. Chem. 36 (1997) 1552.
[7] U.E. Bucher, A. Currao, R. Nesper, H. Rüegger, L.M. Venanzi, E. Younger, Inorg. Chem. 34 (1995) 66.
[8] (a) S. Trofimenko, J.C. Calabrese, J.K. Kochi, S. Wołowiec, F.B. Hulsbergen, J. Reedijk, Inorg. Chem. 31 (1992) 3943. (b) S. Trofimenko, J.C. Calabrese, G.S.Thompson, Inorg. Chem. 26 (1987) 1507. (c) S. Trofimenko, J.C. Calabrese, J.S. Thompson, Inorg. Chem. 31 (1992) 974.
[9] F. Malbosc, P. Kalck, J.-C. Daran, M. Ethienne, J. Chem. Soc. Dalton Trans. (1999) 271.
[10] (a) S. Kiani, J.R. Long, P. Stavropoulos, Inorg. Chim. Acta 263 (1997) 357. (b) A.E. Corrochano, F.A. Jalón, A. Otero, M.M. Kubicki, P. Richard, Organometallics 16 (1997) 145.
[11] (a) M. Akita, K. Ohta, Y. Takahashi, S. Hikichi, Y. Moro-oka, Organometallics 16 (1997) 4121. (b) C.K. Ghosh, W.A.G. Graham, Inorg. Chem. 30 (1991) 778. (c) M. Cocivera, G. Ferguson, B. Kaitner, F.J. Lalor, D.J. O'Sullivan, M. Parvez, B. Ruhl, Organometallics 1 (1982) 1132. (d) U.E. Bucher, A. Currao, R. Nesper, H. Rüegger, L.M. Venanzi, E. Younger, Inorg. Chem. 34 (1995) 66. (e) R.G. Ball, C.K. Ghosh, J.K. Hoyano, A.D. McMaster, W.A.G. Graham, J. Chem. Soc. Chem. Comm. (1989) 341. (f) M. Akita, K. Ohta, Y. Takahashi, S. Hikichi, Y. Moro-Oka, Organometallics 16 (1997) 4121.
[12] (a) E. Del Ministro, O. Renn, H. Rüegger, L.M. Venanzi, U. Burckhardt, V. Gramlich, Inorg. Chim. Acta 240 (1995) 631. (b) N.G. Connelly, D.J.H. Emslie, B. Metz, A.G. Orpen, M.J. Quayle, Chem. Commun. (Cambridge) (1996) 2289.
[13] (a) M.C. Keyes, V.G. Young, W.B. Tolman, Organometallics 15 (1996) 4133. (b) W.J. Oldham, D.M. Heinekey, Organometallics 16 (1997) 467. (c) V. Chauby, C. Serra Le Berre, Ph. Kalck, J.-C. Daran, G. Commenges, Inorg. Chem. 35 (1996) 6354.
[14] (a) C.K. Ghosh, W.A.G. Graham, J. Am. Chem. Soc. 109 (1987) 4726. (b) A.A. Purwoko, A.L. Lees, Inorg. Chem. 35 (1996) 675. (c) A.A. Purwoko, S.D. Tibensky, A.J. Lees, Inorg. Chem. 35 (1996) 7049. (d) S. Zarić, M.B. Hall, J. Phys. Chem. A 102 (1998) 1963. (e) D.D. Wick, T.O. Northcutt, R.J. Lachicotte, W.D. Jones, Organometallics 17 (1998) 4484. (f) D.D. Wick, W.D. Johnes, ibid. 18 (1999) 495. (g) D.D. Wick, K.A. Reynolds, W.D. Jones, J. Am. Chem. Soc. 121 (1999) 3974. (h) H. Katayama, K. Yamamura, Y. Miyaki, F. Ozawa, Organometallics 16 (1997) 4497.
[15] A.L. Rheingold, R. Ostrander, B.S. Haggerty, S. Trofimenko, Inorg. Chem. 33 (1994) 3666.
[16] G.M. Sheldric, SHELX-86 and SHELXL-93, Programs for Crystal Structure Determination, Univertsität Göttingen, Germany, 1986, 1993.
[17] E. Keller, Program SHAKAL, Universität Freiburg, Germany, 1993.
[18] F.A. Cotton, G. Wilkinson, in: Advanced Inorganic Chemistry, fifth ed., Wiley, London, 1988, p. 1299.